Proceedings of the ASME 2012 International Mechanical Engineering Congress & Exposition
IMECE2012
November 9-15, 2012, Houston, Texas, USA

IMECE2012-88572

DESIGN OF A HORIZONTAL AXIS WIND TURBINE FOR FIJI

Jai. N Goundar
The University of the South Pacific
Suva, Fiji
goundar_j@usp.ac.fj

Sumesh Narayan
The University of the South Pacific
Suva, Fiji
narayan_su@usp.ac.fj

Mohammed Rafiuddin Ahmed
The University of the South Pacific
Suva, Fiji
ahmed_r@usp.ac.fj

ABSTRACT

The demand and cost of electricity has increased for Pacific Island Countries (PICs). The electricity from main grid does not reach rural areas and outer islands of Fiji. They burn fuel for electricity and daily lighting. Therefore, there is a need to look for alternative energy sources. Wind turbine technology has developed over the past years and is suitable for generating electricity by tapping wind energy. However, turbines designed to operate at higher wind speed do not perform well in Fiji, because Fiji's average wind velocity is around 5-6 m/s. A 10 m, 3-bladed horizontal axis wind turbine is designed to operate at low wind speed, cut in speed of 3 m/s, cut off speed of 10 m/s and rated wind speed of 6 m/s. The blade sections were designed for different locations along the blade. The airfoil at the tip (AF0914) a has maximum thickness of 14% and maximum camber of 9%; the thickness varies linearly to the root, at the root the airfoil (AF0920) has a maximum thickness of 20% and maximum camber of 9%. The aerodynamic characteristics of airfoil AF0914 were obtained using Xfoil and were validated by experimentation, at turbulence intensities (Tu) of 1% and 3%, and a Reynolds number (Re) of 200,000. The aerodynamic characteristics of other airfoils were also obtained at operating Re at the turbulence intensities of 1% and 3%. These airfoils have good characteristics at low wind speed, and were used to design the 10 m diameter 3-bladed HAWT for Fiji. The turbine has a linear chord distribution for easy manufacturing purpose. Twist distribution was optimized using Blade Element Momentum (BEM) theory, and theoretical power and turbine performance were obtained using BEM theory. At the rated wind speed of 6 m/s and a TSR of 6.5, the theoretical efficiency of the rotor is around 46% and maximum power is 4.4 kW. The turbine has good performance at lower wind speeds and is suitable for Fiji's conditions.

INTRODUCTION

The cost and the demand of electricity for Fiji have increased over the years. Fiji Electricity Authority used about 60,140 tonnes of Industrial diesel oil and Heavy fuel oil to cater for 50% of electricity needs in 2001 [1]. The fuel cost has increased and will continue to increase; also burning fossil fuel emits green house gases, causing global warming and other environmental problems. The electricity from main grid does not reach other islands and some parts of rural areas. Diesel generators are used at these places, but it is not a good solution, it costs even high to transport fuel to these places. Renewable energy resources could be an alternative energy source; it is a clean and green energy source. Today one of the fundamental quests is to produce power using sustainable methods to cater for the problems such as global warming, climate change, pollution, etc. Wind turbines are promising renewable energy devices for harnessing energy from winds. However, a wind turbine designed to operate at higher wind speed and does not perform well at lower wind speeds.

The average wind speeds range in Fiji is around 4 - 6 m/s for most of the areas and the annual average is around 5 - 6 m/s

depending on location (off shore and on mountains) [2]. There is need to design turbines which can operate at low wind speed and have good performance. Work has been done in the area of designing blade sections for turbines which operate at lower velocities [3].

For better performance of turbine, airfoils with good aerodynamic characteristics must be used. The commonly used NACA airfoils are not appropriate for turbines designed for low wind speeds and many researchers have worked on developing new low wind speed airfoils to extract maximum power from wind [2.4-5]. One of the most important components of the wind turbine is its rotor blade and hence a careful analysis needs to be performed such as distribution of chords, twists and the selection of the wind turbine [6]. Wang et al. [7] developed a domestic wind turbine with scoop for build up areas and predicted its annual power output. The performance enhancement with the installed scoop was unknown. Sharma and Madawala [8] analyzed a smart wind turbine with variable length blades. Further, they proposed an innovative hybrid mechanical-electrical power conversation system. When the wind speeds fall below the rated wind speed the variable length blade wind turbine diameter is extended and the annual energy output of such turbine is almost doubled to that of a corresponding turbine with fixed length.

In order to successfully design a wind turbine rotor, it is important to understand the aerodynamics of the rotating blades. Various parameters must be considered while designing rotors such as: stall characteristics, blade torque and power, airfoil characteristics: c_l, c_d and pressure distribution. Airfoils are most important part of the rotor, the rotor performance depends on airfoil characteristics. c_l and c_d are the most important characteristics of airfoil, the local c_l and c_d on the blade changes with varying wind speed and changing local α of airfoils. Therefore, c_l is maximized and c_d is kept as low as possible to maximize the turbine performance. Also a delayed stall is desirable on airfoils. The c_l and c_d can be determined by experimentation or using XFoil. XFoil is a linear vorticity stream function panel method with viscous boundary layer and wake model, and is suitable for predicting 2-D airfoil characteristics [9]. The theoretical performance of the rotor can be easily predicted using Blade element momentum (BEM) theory. BEM theory is based on the Glauert propeller theory [10]. By applying the momentum and angular momentum conservation equations and feeding in the 2-D airfoil characteristics c_l and c_d, the torque and power on the shaft can be easily obtained. In recent years, BEM theory has been modified and optimized to give good results [11].

This paper presents the design of new airfoil series for different location of blade radius, generally thick airfoils are required at the blade root to hub connection of the blade and thin airfoil near the tip of the blade. The airfoil series was named as AF09XX. The characteristics of the airfoils were determined at its operating Re at rated wind speed of 6m/s, and the characteristics was compared at different Tu of 1% and 3%. Changing turbulence intensity often affects the turbine performances. The new section has good characteristics at low wind speed. These sections are used to design a 10 m, 3-bladed rotor for Fiji. The blade chord distribution was optimized using Blade element momentum (BEM) theory and the theoretical power output and efficiency were determined using BEM theory. The rotor has maximum theoretical efficiency 46% and theoretical maximum power 4.4 kW at TSR of 6.5 and rated wind speed of 6 m/s.

NOMENCLATURE

a	axial flow induction factor
a'	tangential flow induction factor
A	rotor area (m^2)
c	chord (m)
c_d	Drag Coefficient ($D/½\ \rho AV_r^2$)
c_l	Lift Coefficient ($L/½\ \rho AV_r^2$)
C_P	Coefficient of pressure ($P_L - P\infty)/(\ 0.5\rho V_r^2$)
D	Drag (N)
g	acceleration due to gravity (m/s^2)
k	is constant (k > 0)
L	Lift (N)
P	rotor Power (W)
P_L	Local Pressure (N/m^2)
P_∞	freestream static pressure (N/m^2)
r	radius of local blade element (m)
R	blade radius (m)
t	maximum thickness of airfoil (m)
T	rotor trust (N)
Tu	turbulence intensity
U_o	uncorrected freestream velocity (m/s)
V_r	relative velocity of rotating blade $\sqrt{U_o^{\,2}(1-a)^2+\Omega^2 r^2(1+a')^2}$
α	angle of attack of the water flow on the hydrofoil
ρ	density of air (Kg/m^3)
ε^{sb}	solid blockage correction factor
K_1	wind-tunnel correction constant for solid blockage effects (0.74)
M_v	model volume (m^3)
Ω	rotational speed (rad/s)
C_{Pw}	Power coefficient = $P/(0.5\rho AV_r^2)$
β	angle of twist
α_t	$(\varphi - \beta_t) + \alpha_o$
φ	$\tan^{-1}(U_o/V_t)$
β_t	angle of twist at tip (0°-2°)
α_o	zero lift angle of attack

DESIGN OF AIRFOILS AND THEIR CHARACTERISTICS AT OPERATING REYNOLDS NUMBER

Aerodynamic characteristics of airfoils that must be studied while designing include the pressure distribution on the airfoil surface, the minimum coefficient of pressure (C_P), coefficient of lift (c_l), coefficient of drag (c_d), and lift to drag ratio (L/D). An important challenge many researchers face is designing an airfoil with high L/D ratio at high angles of attack and delayed stall. This is important since higher turbulence and higher relative velocity are experienced than the usual turbulence and relative velocity. Further, the relative velocity experienced by the turbine blade varies from root to the tip of the turbine blade. The airfoils for different blade section were designed from existing S1210 series airfoil by modifying the maximum camber and maximum thickness; this was done after studying the aerodynamic characteristics of several best performing airfoils and modifying its geometry, such as varying nose radius, maximum camber, maximum thickness and trailing edge thickness. The three modified airfoil performed better for the aforementioned airfoil characteristics and hence, chosen in this present work. The sections were named as AF09XX series, 09 denotes that the airfoils have maximum camber of 9% and XX denotes the maximum thickness of the blade section along the blade.

A thick airfoil was designed for the root region which has a maximum thickness of 18%; it is named AF0918. For the blade tip a thinner airfoil was designed, which has a maximum thickness of 14%. This airfoil is named AF0914. For the mid-section of the blade, an airfoil of maximum thickness of 16% is designed and named AF0916. All the three airfoils have a maximum camber of 9%. The maximum thickness of the blade section varies linearly from root to the tip for easy merging of blade surface. The airfoils used and the maximum thickness along the blade are shown in Table 1. The geometry of the airfoil AF0914 is shown in Fig. 1, AF0916 and AF0918 have similar geometry to that of AF0914, only the maximum thickness is different.

Table 1: Airfoils and their thickness distribution along the blade.

r/R	t/C	Airfoil
0.2	18	AF0918
0.3	17.5	
0.4	17	
0.5	16.5	
0.6	16	AF0916
0.7	15.5	
0.8	15	
0.9	14.5	
1	14	AF0914

The airfoils were tested in an Engineering Laboratory Design Inc. open circuit, suction type, low speed wind tunnel in the Thermo-fluids laboratory at the University of the South Pacific. This wind tunnel has a single stage centrifugal flow fan which capable of producing airflows up to 48.77 m/s in the test section of size 303 mm x 303 mm x 1000 mm. The corrected airflow was discharged into the test section through the square outlet of the contraction with the area ratio of the contraction nozzle of 6.25:1 via a settling chamber consisting of honeycomb gauges and three high porosity screens.
Solid blockage caused by the walls of the test section increases the flow velocity in the test section. The solid blockage was corrected using the equations 1 and 2 [12].

$$V = V_u\left(1 + \varepsilon^{sb}\right) \quad (1)$$

$$\varepsilon^{sb} = \frac{k_1\left(m_v\right)}{(csa)^{\frac{3}{2}}} \quad (2)$$

Airfoil AF0914 was fabricated with 30 pressure taps on the upper and lower surfaces to measure the pressure distribution using a Furness Controls Micromanometer (model FCO510) having a range of ± 19620 Pa. The AF0914 airfoil investigated in this work has a maximum thickness of 14%, maximum camber of 9%, and a chord length of 100 mm.
Experiments were carried out at Re of 200,000 based on the chord length and corrected freestream velocity. The turbulence intensity (Tu) in the test section is of the order of 1% for the above-mentioned Re. The pressure taps were located near the mid-span of the airfoil of length 300 mm. The airfoil was placed with the leading edge 10 cm from the inlet of the test section to ensure a two-dimensional flow over the pressure taps. The turbulence intensity was increased by removing one of the screens of the wind tunnel. The angle of attack (α) was varied from 0^o to 20^o in increments of 2^o and the pressure reading were recorded for the 30 pressure taps located on the airfoil surface. From the pressure readings, the C_p values were calculated. The accuracy of C_P measurements was estimated to be ±1.9%, while the repeatability was ±1.82%. Another AF0914 airfoil was manufactured without pressure taps to measure the lift and drag.

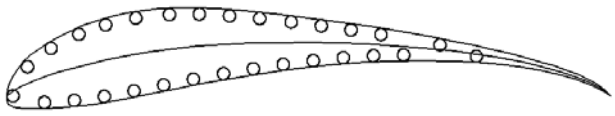

Fig. 1: Airfoil AF0914 with location of pressure taps.

RESULTS AND DISCUSSION

The results are presented and discussed in this section. Figures 2 and 3 compare the numerical and experimental pressure distributions on the AF0914 airfoil tested at Re = 200,000. The Cp is calculated for α of 6° and 10° at Tu of 1% and 3%. From Figs. 2 and 3, it can be seen that the suction peak predicted by Xfoil is slightly lower for Tu of 1%. Further, the value of experimental C_P on the upper surface are slightly higher compared to the Xfoil results. The C_P values on lower surface and the suction on the upper surface decreases as the Tu increase. Overall, there is a good agreement between the experimental and numerical C_P values.

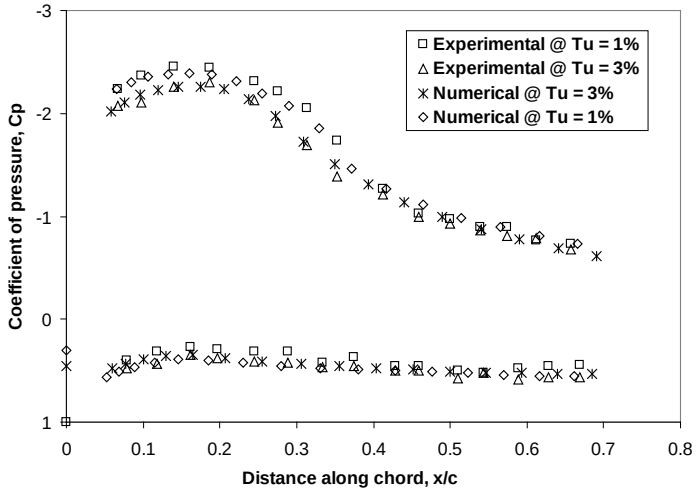

Fig. 2: Comparison of numerical and experimental pressure distributions on the AF0914 airfoil surface for α of 6° and Re of 200,000.

Figure 4 shows the comparison of Xfoil and experimental values of c_l at different α for Re = 200,000. For Tu of 1% Xfoil slightly over predicts c_l and shows slightly delayed stall, whereas for Tu of 3% experimental results shows a delayed stall. As seen there is a good agreement between the Xfoil results before stall α. XFoil predicts Lift and drag using panel method, which gives good prediction just before maximum lift [13]. XFoil does not give good prediction at higher angles of attack in the presence of a thick wake and for early separation. This could be the main reason for the discrepancy of XFoil and experimental results after maximum lift.

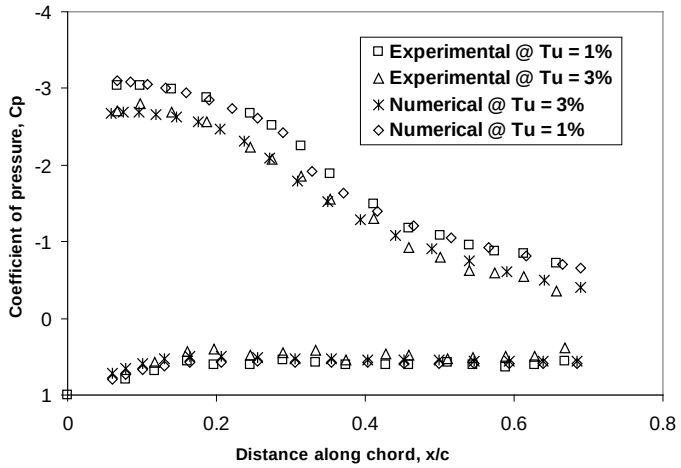

Fig. 3: Comparison of numerical and experimental pressure distributions on the AF0914 airfoil surface for α of 10° and Re of 200,000.

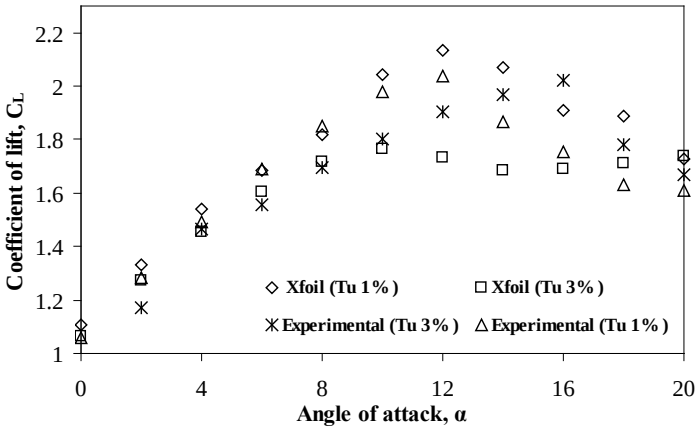

Fig. 4: Comparison c_l for AF0914 airfoil at different α, and Re of 200,000.

Overall the experimental values of coefficient of pressure (Figs. 2 & 3) and the coefficient of lift (Fig. 4) are in good agreement with the Xfoil predicted results.

The aerodynamic characteristics of AF09XX airfoil series at Re, 0.4 million (0.4M) – 0.65 million (0.65M) were obtained from XFoil, that is at operating U_o of 6m/s. The c_l and c_d varies with α, the airfoils have good aerodynamic characteristics at certain range of α, but at one α airfoils give their best characteristics and it is called optimum angle of attack. The optimum α needs to be determined, to compare the characteristics of airfoils. The optimum α for any airfoil can be determined using polar plots of c_l and c_d. From the polar plots of AF09XX series airfoils at its operating Re (Fig. 5), the optimum α of AF0914, AF0916 and AF0918 is around 12˚. Taking into account the variation in the flow conditions due to turbulence, settling of dust or dirt on the blade surface, etc., the optimum operating α chosen is usually few degrees less than

this point, therefore, the optimum α for AF09XX series is chosen as 10˚.

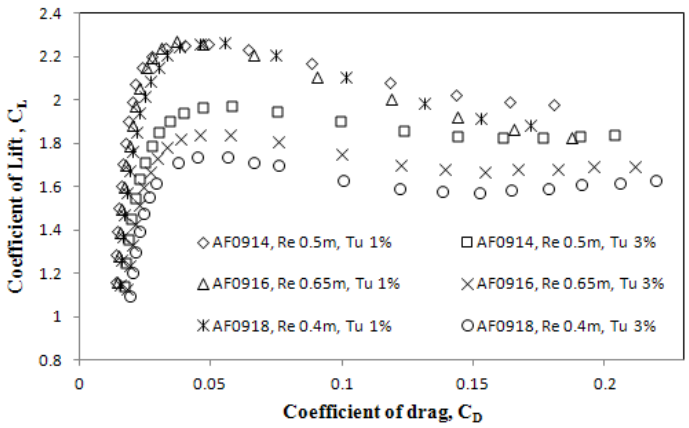

Fig. 5: Polar plot of c_l and c_d of AF09XX series airfoils at Tu of 1% and 3%.

Lift plays a significant role in enhancing the performance of the turbine and one of the important tasks while designing a HAWT is to maintain L/D ratio high as possible, especially from the mid section to blade tip, because this part of the blade contributes to 70-80% of the total power of the rotor. A graph of c_l against α is plotted as shown in Fig. 6 for AF09XX airfoils. All the airfoils have their maximum c_l of approximately 2.1 at an optimum α of 10^o at Tu of 1%.

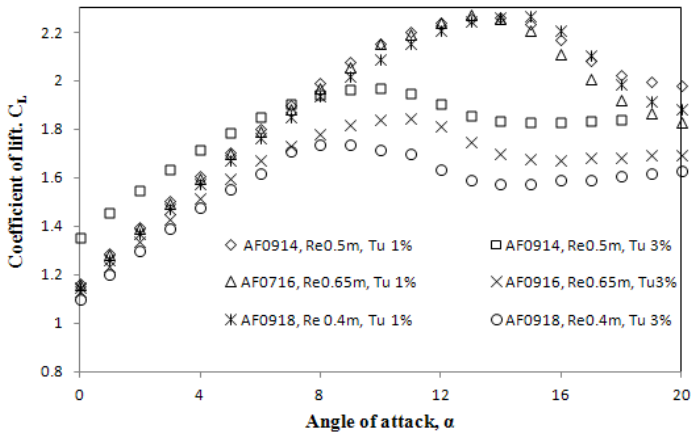

Fig. 6: Coefficient of lift c_l at different α, of AF09XX airfoils at Tu of 1% and 3%.

The root section airfoil AF0918 is tested at Re = 0.5M, mid section airfoil AF0916 is tested at 0.6M and the tip section airfoil AF0914 is tested at 0.7M. Further, the airfoils maintain higher c_l over a wide range of α from 8° - 16° at Tu of 1%, the turbine will be able to maintain its performance at changing wind velocities, which normally alters the local α. The c_l slightly increases for AF0914 at Tu of 3% from 0 - 8° α, and c_l decreases for AF0916 and AF0918 at 3% Tu predicted by Xfoil. But overall all airfoils have higher c_l of around 1.8 at 10° and Tu of 3%. The c_l decreases rapidly after stall α for AF0918 airfoil, this section is mainly for strength purpose.

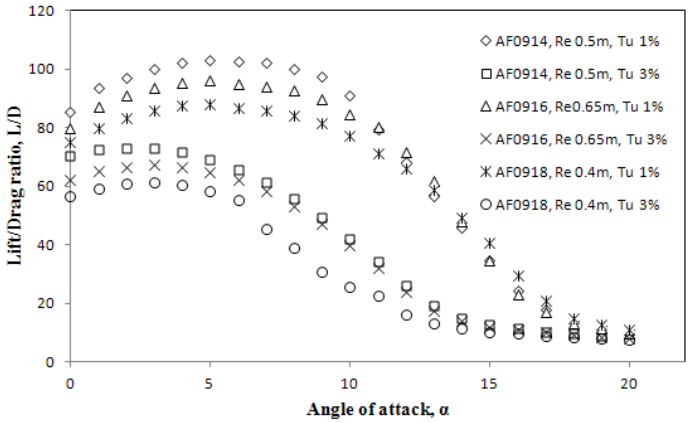

Fig. 7: L/D ratio of AF09XX airfoils at different α, and Tu of 1% and 3% at its operating Re.

Lift to drag ratio is also very important in design of HAWT, for good performance of the turbine, the L/D ratio of airfoils are always maximized. The airfoils must have higher L/D over a wide range of α so that the rotor performance is not affected in changing wind and turbine operating conditions. The L/D ratios for all the airfoils at different α are shown in Fig. 7. At operational α of 10° the L/D ratio is in the range of 78 - 92 for all the airfoils at lower Tu. The airfoil maintains high L/D ratio till 12° - 14° at Tu of 1%. At Tu of 3% the L/D ratio decreases. It is around 50 for AF0914 and AF0916, and slightly lower for AF0918, which is around 25.

All the airfoils have higher L/D over a wide range of α and at both the Tu, therefore, the turbine will maintain its efficiency at changing wind condition and varying Tu.

LOCATION OF TRANSITION POINT

The boundary layer (BL) on the upper surface of the airfoil change from laminar to turbulent, the point at which boundary layer changes is called the transition point. It is very important to study the location of the transition point (TP) on the upper surface of the airfoil used for wind turbines. The location of TP mostly depends of airfoil geometry itself; however the TP shifts either towards trailing edge (TE) or leading edge (LE) with changing Re, Tu, surface roughness and at different α [14]. The freestream turbulence levels of atmospheric wind at which wind turbines operate are usually higher than the levels achieved in wind tunnels and vary for different locations. The Tu is usually low at offshore locations. The varying Tu affects the turbine performance; therefore it is important to study how the location

of TP varies at with changing Tu. Also the dirt and dust gets on the blades surface, this causes early transition of BL, and this reduces the $c_{l\,max}$ [15].

The distance from the LE to the point where transition occurs is denotes as x_{tr}. As x_{tr} reduces, the region of laminar boundary layer reduces and the region of turbulent boundary increases, this results in increase friction, however there is reduction in wake thickness reducing the pressure drag.

The location of TP can be determined from pressure distribution around airfoil optained from XFoil. A kink in the C_P plot denotes the location of the transition point. The C_P of airfoils AF09XX series at Tu of 1% and 3% and at 3 different Re at U_o of 3 m/s, 6 m/s and 10 m/s are shown in Figs 8-10.

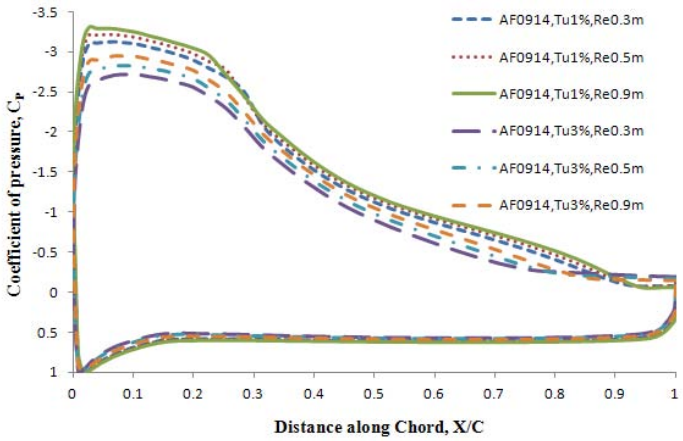

Fig. 8: Pressure distributions on the AF0914 airfoils for α of 10^o at its operating Re and Tu of 1% and 3%.

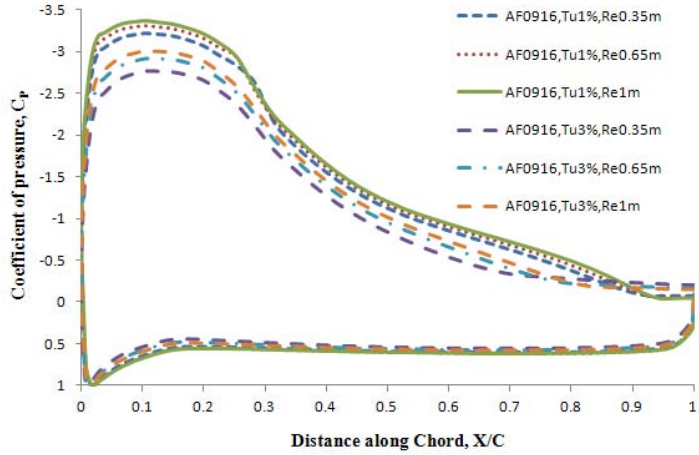

Fig. 9: Pressure distributions on the AF0916 airfoils for α of 10^o at its operating Re and Tu of 1% and 3%.

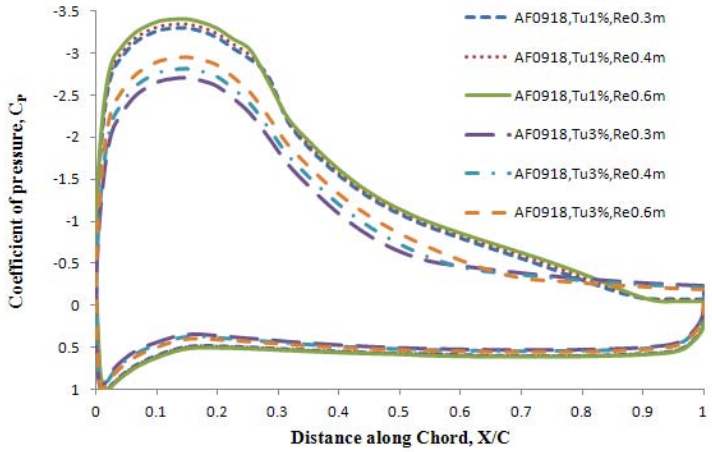

Fig. 10: Pressure distributions on the AF0916 airfoils for α of 10^o at its operating Re and Tu of 1% and 3%.

Figure 8 shows the TP at different operating Re and Tu of 1% and 3% on AF0914 airfoil. For AF0914 x_{tr} decreases with increasing Re and increasing Tu. At Tu of 1%, TP is around 0.25 - 0.28 of x/C for Re between 0.3m and 0.9m and for Tu of 3%, the XFoil results show TP shifts very close to LE (0.02 of x/C). Similar trends are seen for airfoils AF0916 and AF0918 shown in Figs 9-10, at Tu of 1% the TP is around 0.25 – 0.29 of x/C at Re between 0.35m to 1m for AF0916 and Re between 0.3m - 0.6m for AF0918. The TP shifts very close to LE around 0.02 x/C. The transition point is close to LE for all airfoils, therefore, the blade performance will not be affected much in changing Tu and surface roughness.

DESIGN OF 3-BLADED, 10 M HORIZONTAL AXIS WIND TURBINE ROTOR

Turbines with bigger diameter produce more power. As we increase the diameter the cost of turbine and structure increases, the main problem arises when there is need to bring the turbine down for maintenance or during strong winds, especially for Fiji, where the cyclone season lasts for 6 months. A 10 m wind turbine will be more appropriate for Fiji. Wind turbines mostly have 2 or three blades, there is slight increase in power when moving from 2 blades to 3 blades, however, 3-bladed turbines are more stable, and require less maintenance [16]. Therefore, a 3-bladed, 10 m rotor was designed, the rated design wind speed is 6 m/s, cut in speed of 3 m/s and cut of speed of 10 m/s.

The blades were designed using AF09XX series airfoil sections. For good aerodynamic efficiency the chord distribution must follow the hyperbolic curve, for manufacturing point of view the chord distribution is usually linear. Equation 3 gives theoretically optimum chord distribution for the turbine blade [16].

$$C_{opt} = \frac{2\pi r}{z} \frac{8}{9C_L} \frac{V_{wd}}{TSR(V_r)} \qquad (3)$$

However, the chord distribution is modified for optimum efficiency and blade strength. The optimized chord distribution for the blade is shown in Fig. 11.

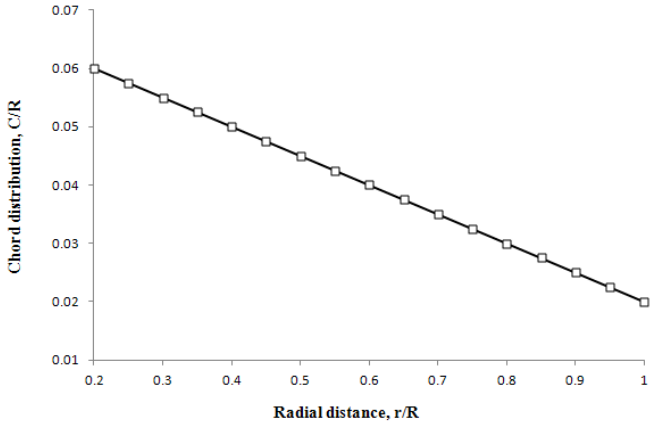

Fig. 11: Chord distribution of turbine blade

The operating TSR for 3-bladed rotors is usually between 6-8, the optimum TSR for the rotor is 6.5. Another important factor that must be taken into account is rotor solidity. The theoretical rotor solidity for 3-bladed rotors operating at TSR of 6.5 is around 5%. The solidity for the designed rotor is around 3%, this was slightly modified for optimum chord distribution. The thickness distribution of airfoils from root to tip also plays important role in blade strength and rotor performance. Thin airfoils have good aerodynamic characteristics, therefore thin airfoils are required from tip to midway of the blade. The maximum power is generated at this section. The root section doesn't produce much power, so the main priority of the root section is given towards blade strength; therefore, thick airfoils are used near root. Linear thickness distribution was used from tip to root, 14% of t/C at r/R =0 (tip) to 18% of t/C (root).

The V_t increases from root to tip of the blade, this results in increase in V_r and this result in change in local α along the blade for untwisted blade, therefore, the blade needs to be twisted. The theoretical optimum twist of blade can be calculated using equation 4 [17].

$$\beta = (R/r\alpha_t - \alpha_t) - k(1-r/R) \qquad (4)$$

The twist distribution for the blade was slightly modified, to optimize its performance at low wind speed and TSR of 6.5. The optimized twist distribution of the designed rotor is shown in Fig. 12.

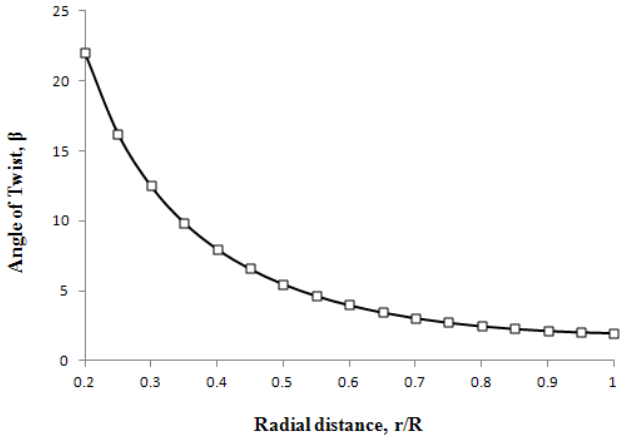

Fig. 12: Twist distribution of turbine blade.

PERFORMANCE ANALYSIS OF ROTOR

The performance of rotor blade is measured by the amount of power it delivers during rotation with theoretical power available in the wind passing through the same area swept by the blade. The maximum theoretical efficiency of wind turbine can be 59.2 % according to Betz criteria , but in practice the average efficiency of HAWT reaches to 40 - 45% [18]. Apart from maximum efficiency, it is important that turbine maintain high efficiency at wide range of TSR. The sudden change U_o alters the operation TSR of rotors; therefore, the turbine should perform well in changing U_o. The theoretical efficiency of the rotor can be predicted using BEM theory [11]. The main turbine parameters that must be fed in the theory is the airfoil characteristics c_l and c_d at different α and at operating Re, other parameters are wind velocity, the turbine radius, chord distribution, and twist distribution to calculate local α and blade forces, and finally computing the rotor power. The results of power prediction using BEM theory was experimentally verified in ref [19] and shows good agreement between experimental and theoretical results. The rotor performance was determined using BEM as shown in Fig. 13. It shows the rotor gives maximum efficiency of 46% at TSR of 6.5, furthermore, rotor maintains higher efficiency from TSR of 5.5 to 7.5. Therefore, turbine will maintain its efficiency at changing turbine operating conditions.

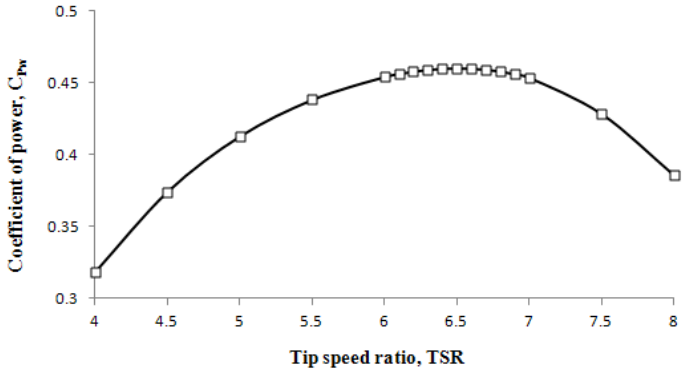

Fig. 13: Efficiency of rotor, at different TSR, the rotor follows same efficiency curve at wind speed of 3-10 m/s.

The theoretical power of the rotor was also obtained using BEM theory, as shown in Fig. 14. The theoretical maximum power at cut in wind speed of 3 m/s is around 0.6 kW at TSR of 6.5, at rated wind speed of 6 m/s maximum power is around 4.5 kW and around 20 kW at cut of wind speed of 10 m/s. Overall the rotor has good efficiency at low wind speed, and it is appropriate for Fiji's wind conditions.

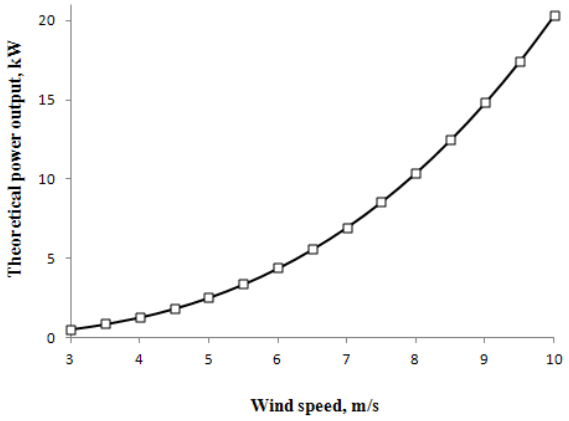

Fig. 14: Theoretical power output, from cut in wind speed 3 m/s to cut off wind speed of 10 m/s.

CONCLUSION

The present work involves designing of new airfoils for a low wind speed turbine. The blade sections designed were named AF09XX series airfoils. These airfoils have good aerodynamic characteristic at both 1% and 3% Tu. All the airfoils meet the criteria of high L/D and c_l over a wide range of α at changing Tu; furthermore, the thick sections near root will provide strength to the blades. These airfoils were designed for a 3-bladed 10 m wind turbine rotor. The rotor is designed to operate in low wind conditions in Fiji. The maximum theoretical efficiency predicted using BEM theory of the rotor is around 46% at the TSR of 6.5, and the maximum power at the rated wind speed of 6 m/s is around 4.4 kW. Wind farms in Fiji with similar turbines could solve electricity problems faced by the country.

ACKNOWLEDGMENTS

The authors would like to acknowledge the help rendered by Mr. Sanjay Singh, lab Technician at the University of the South Pacific and Mr. Frank Daukalia, Mr. Ameniasi Naiqamu, and Mr James Koronaa, final year students, 2011, for helping in the fabrication of the airfoils and during experimentation.

REFERENCES

[1] "Fiji Electricity authority; annual report 2010," Fiji electricity authority 2011.

[2] Ahmed, M.R., Narayan, S., Zullah, M.A., Lee, Y.H., 2011, "Experimental and numerical studies on a low Reynolds number airfoil for wind turbine blades", Journal of Fluid Science and Technology, **6**, pp. 357-371.

[3] Singh, R.K., Ahmed, M.R., Zulla, M.A., Lee, Y.H., 2011, "Design of a low Reynolds number airfoil for small horizontal axis wind turbines", Renewable energy.

[4] Yasunari, K., Takao. M., Junuke. M., Tatsuya.T., Akira., 2011, "Effects of turbulence intensity on dynamic characteristics of wind turbine airfoil", Journal of Fluid Science and Technology, **6**, pp. 333-341.

[5] Yasuo, H., Nobukazu. T., Chin-Hoh. M., Hitoshi. S., Shuji. I., Yuzuru. E., Hiromaru. H., Soichiro. S., 2011, "Numerical simulation of atmospheric turbulence for assesment of wind turbine", Journal of Fluid Science and Technology, **6**, pp. 342-356.

[6] Xuan, H., Weimin. Z., Xiao. L., Jeiping. L., 2008, "Aerodynamic and Aeroacoustic Optimization of Wind Turbine Blade by a Genetic Algorithm", in AIAA Aerospace Sciences Meeting and Exhibit, Reno, Nevada, pp. 1331.

[7] Wang, F., Bai. L., Whiteford. J., Cullen. D., 2008, "Development of small domestic wind turbine with scoop and prediction of its annual power output", Renewable Energy, **33**, pp. 1637-1651.

[8] Sharma, R.N., Madawala, U.K., 2010, "The concept of a smart wind turbine system", Renewable Energy, **39**, pp. 403-410.

[9] Drela, M., 1989, "An analysis and design system for low Reyolds number airfoils", in Conference on Low Reynolds Number Airfoils Aerodynamics, University of Notre Dame.

[10] Glauert, H., 1926, "The elements of airfoil and airscrew theory", Cambridge University Press.

[11] Lanzafame, R., Messina, M., 2007, "Fluid dynamics wind turbine design: Critical analysis, optimization and application of BEM theory", Renewable Energy, **32**, pp. 2291-2305.

[12] Barlow, J.B., Rae. W.H., Pope. J.R., 1999, "Low Speed Wind Tunnel Testing", New York: Wiley Interscience.

[13] Drela, M., 2001, “XFoil 6.94 User Guide” , MIT Aero & Astro Harold Youngren, Aerocraft, Inc.

[14] Ahmed. M.R, 2012 "Blade sections for wind turbine and tidal current turbine applications - current status and furure challeges," International Journal of Energy Research,**36**, pp. 829-844.

[15] Abbott. I. H., Doenhaff. A.E.V., 1959 "Theory of wing sections", New York: Dover Publication Inc.

[16] Hau, E., 2006, "Wind Turbines; Fundamentals, Technologies, Application, Economics", Germany: Springer.

[17] Habali, S.M., Saleh, I.A., 1994, "Design and testing of small mixed airfoil wind turnbine blade", Renewable Energy, **6**, pp. 161-169.

[18] Ozener, O., Ozener, L., 2006, "Exergy and Reliablity analysis of wind turbine system: A case study", Renewable and sustainable Energy Reviews, **11**, pp. 1811-1826.

[19] Shen, X., Zhu. X., Du. Z., 2011, "Wind turbine aerodynamics and loads control in wind shear flow", Energy, **36**, pp. 1424-1434.